Proceedings of the 28th IEEE
EMBS Annual International Conference
New York City, USA, Aug 30-Sept 3, 2006

A Localization Method Using 3-axis Magnetoresistive Sensors for Tracking of Capsule Endoscope

Xiaona WANG, *Student Member, IEEE*，Max Q.-H. MENG, *Senior Member, IEEE*, and Chao HU, *Member, IEEE*

***Abstract* - In this paper, we propose a non-invasive tracking method, which has the potential to be used for localization of the capsule endoscope. The tracking system consists of a magnetic marker, a sensor array, amplifiers, data acquisition devices and a signal processing unit. The marker is modeled as a magnetic dipole to simplify the theoretical expression of the magnetic field distribution. By minimizing the squared error of the field values between the calculation and measurements using Levenberg-Marquardt optimization method, the 5 localization parameters of the dipole can be determined. Real time experiments were carried out to test the feasibility of the method. It is demonstrated that, the accuracy of the localization is related to the number of sensors. For the sensor array including 16 3-axis magnetoresistive sensors, the average position error is 3.3mm and the average orientation error is about 3°, when the magnetic marker is 100mm above the sensor array plane.**

I. Introduction

Wireless capsule endoscope [1] is a great advancement in the history of endoscopy. It gets rid of the tedious and cumbersome insertion procedures of the traditional endoscope, reduces the patients' pain and allows the examination of the whole small intestine. However, because of the passive locomotion pattern, it takes a long time (20-36 hours) for the capsule to go through the gastrointestinal (GI) tract, thus makes a real-time examination impossible. To facilitate the diagnosis and make a base for a wireless guiding system, it's necessary to know the exact position and orientation of the capsule.

M2A endoscopic system [1] includes a localization module, which is based on the strength of the RF (radio frequency) signals received by the 8 antennas on the exterior of the human abdomen. The average error of this method is about 37.7mm [2], which is not accurate enough for this application. Some image methods, such as CT scan, Ultrasound, MRI, *etc.*, can fulfill the requirement, but these devices are stationary and expensive.

Magnetic field is useful to detect hidden objects and provide low cost system, comparing with image system [3, 4, 5]. It marks not only the 3-D position of the magnetic source, but also the orientation. For human body related localization, permanent magnets are preferred to electromagnetic field, because they are easy to get, convenient to integrate and most importantly, non-invasive. The magnetic localization method had once been employed for monitoring the GI mobility [6-8] and studying the jaw movement [9, 10]. In the previous work [11,12], we've enclosed a cylindrical magnet into a capsule and carried out experiments to test the magnetic motion capture method for capsule tracking. In this paper, the dipole model of the magnetic marker is studied to investigate the error of the method. A real-time localization system, which is based on a combination of the magnetic field measurement and signal-processing technique, is developed and tested.

The paper is organized as following: section II is modeling of the magnetic marker as a dipole; section III introduces the magnetically tracking method; the real-time tracking system and experimental results are depicted in section IV, which is followed by the conclusions in section V.

II. Modeling of Magnetic Marker

Assume the cylindrical magnetic marker enclosed in the capsule has a diameter of R and a length of $2L$, and the magnetization of the magnet is M, then the magnetic moment is the integration of M over of the volume of the marker V:

$$P_m = \int_V M dV = 2\pi R^2 LM \cdot \tag{1}$$

As there's no intrinsical difference between the field generated by a magnet and by a current, we replace the magnet with two identical circular currents to calculate the magnetic field distribution of the marker, which are separated for a distance of $2L$. The permeability of human body is very close to that of the air, so we neglect its influence on the static magnetic field. According to Biot-Savart law, the magnetic field of a current element is calculated by:

$$d\mathbf{B} = \frac{\mu_0}{4\pi}\frac{Id\mathbf{l}\times\mathbf{a}}{a^3}, \tag{2}$$

where $d\mathbf{l}$ is infinitesimal length of conductor carrying electric current I, $\mathbf{a}$ is the vector pointing from the short segment of current to the observation point, and μ_0 is the permeability of air.

As shown in Fig. 1, the magnet is orientated along Z- axis; $P(r_1\sin\theta_1\cos\varphi_1, r_1\sin\theta_1\sin\varphi_1, r_1\cos\theta_1)$ is an arbitrary point in coordinate X_1-Y_1-Z. For the upper circular current, we have

$$d\mathbf{l}_1 = (-R\sin\varphi d\varphi, R\cos\varphi d\varphi, 0) \tag{3}$$

$$\mathbf{a}_1 = (r_1\sin\theta_1\cos\varphi_1 - R\cos\varphi, r_1\sin\theta_1\cos\varphi_1 - R\sin\varphi, r_1\cos\theta_1) \tag{4}$$

then

This project is supported by RGC Competitive Earmarked Research Grant #CUHK4213/04E of the Hong Kong government, awarded to Max Meng.

Xiaona Wang is with the Department of Electronic Engineering, the Chinese University of Hong Kong, Shatin, N.T., Hong Kong (e-mail: xnwang@ ee.cuhk.ed.hk).

Max Q.-H. Meng, was with University of Alberta, Canada. He is now with the Department of Electronic Engineering, the Chinese University of Hong Kong, Shatin, N.T., Hong Kong (e-mail: max@ee.cuhk.edu.hk).

Chao Hu is with the Department of Electronic Engineering, the Chinese University of Hong Kong, Shatin, N.T., Hong Kong (e-mail: chu@ ee.cuhk.ed.hk).

$$d\mathbf{l}_1 \times \mathbf{a}_1 = \begin{vmatrix} i & j & k \\ -R\sin\varphi d\varphi & R\cos\varphi d\varphi & 0 \\ r_1\sin\theta_1\cos\varphi_1 - R\cos\varphi & r_1\sin\theta_1\sin\varphi_1 - R\sin\varphi & r_1\cos\theta_1 \end{vmatrix}. \quad (5)$$

Because

$$|\mathbf{a}_1| = \sqrt{r_1^2 + R^2 - 2Rr_1\sin\theta_1\cos(\varphi-\varphi_1)}, \quad (6)$$

we have

$$a_1^{-3} = \frac{1}{(\sqrt{r_1^2+R^2})^3}\left(1 - \frac{2Rr_1\sin\theta_1\cos(\varphi-\varphi_1)}{R^2+r_1^2}\right)^{-3/2}. \quad (7)$$

As $\left|\frac{2Rr_1\sin\theta_1\cos(\varphi-\varphi_1)}{R^2+r_1^2}\right| < 1$, equation (7) can be extended according to equation (8):

$$(1+x)^m = 1 + mx + \frac{m(m-1)}{2!}x^2 + \ldots \quad (|x|<1). \quad (8)$$

Omit the high-order items, and equation (7) is turned into:

$$a^{-3} = \frac{1}{(\sqrt{r_1^2+R^2})^3}\left[1 - \frac{3Rr_1\sin\theta_1\cos(\varphi-\varphi_1)}{R^2+r_1^2}\right]. \quad (9)$$

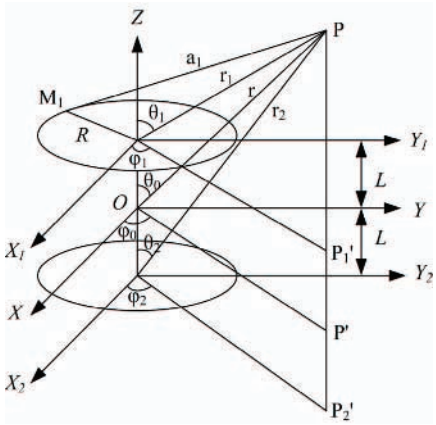

Fig. 1 The permanent magnet oriented along Z-axis is replaced by two circular currents for calculation of the magnetic field at P.

The magnetic flux density $\mathbf{B}_1$ can be decomposed as $\mathbf{B}_1 = B_{x1}\mathbf{i} + B_{y1}\mathbf{j} + B_{z1}\mathbf{k}$. Substitute (5) and (9) into (2) and integrate the current elements, we get the three components:

$$\begin{cases} B_{x1} = \dfrac{3\mu_0}{8\pi}\dfrac{P_m/2}{(\sqrt{R^2+r_1^2})^3}\dfrac{r_1^2\sin 2\theta_1\cos\varphi_1}{(R^2+r_1^2)} \\ B_{y1} = \dfrac{3\mu_0}{8\pi}\dfrac{P_m/2}{(\sqrt{R^2+r_1^2})^3}\dfrac{r_1^2\sin 2\theta_1\sin\varphi_1}{(R^2+r_1^2)} \\ B_{z1} = \dfrac{\mu_0}{2\pi}\dfrac{P_m/2}{(\sqrt{R^2+r_1^2})^3}\left(1 - \dfrac{3}{2}\dfrac{r_1^2\sin^2\theta_1}{R^2+r_1^2}\right) \end{cases} \quad (10)$$

Using similar method, we can get the magnetic field of the lower circular current $\mathbf{B}_2 = B_{x2}\mathbf{i} + B_{y2}\mathbf{j} + B_{z2}\mathbf{k}$. The total magnetic field is superposition of the upper and lower ones:

$$\mathbf{B} = (B_{x1}+B_{x2})\mathbf{i} + (B_{y1}+B_{y2})\mathbf{j} + (B_{z1}+B_{z2})\mathbf{k}, \quad (11)$$

so

$$\begin{cases} B_x = \dfrac{3\mu_0 P_m/2}{8\pi}\left[\dfrac{r_1^2\sin 2\theta_1\cos\varphi_1}{(R^2+r_1^2)^{5/2}} + \dfrac{r_2^2\sin 2\theta_2\cos\varphi_2}{(R^2+r_2^2)^{5/2}}\right] \\ B_y = \dfrac{3\mu_0 P_m/2}{8\pi}\left[\dfrac{r_1^2\sin 2\theta_1\sin\varphi_1}{(R^2+r_1^2)^{5/2}} + \dfrac{r_2^2\sin 2\theta_2\sin\varphi_2}{(R^2+r_2^2)^{5/2}}\right] \\ B_z = \dfrac{\mu_0 P_m/2}{2\pi}\left(\dfrac{2(R^2+r_1^2)-3r_1^2\sin^2\theta_1}{2(\sqrt{R^2+r_1^2})^5} + \dfrac{2(R^2+r_2^2)-3r_2^2\sin^2\theta_2}{2(\sqrt{R^2+r_2^2})^5}\right) \end{cases} \quad (12)$$

From Fig. 1, we have the following geometrical relationships:

$$\begin{cases} r\cos\theta_0 = r_1\cos\theta_1 + L = r_2\cos\theta_2 - L \\ r\sin\theta_0 = r_1\sin\theta_1 = r_2\sin\theta_2 \\ r_1^2 = L^2 + r^2 - 2Lr\cos\theta_0 \\ r_2^2 = L^2 + r^2 + 2Lr\cos\theta_0 \\ \varphi_0 = \varphi_1 = \varphi_2 \end{cases} \quad (13)$$

Substitute equation (13) into (12); replace the parameters with r, θ_0, φ_0, which express the position of P in *O-X-Y-Z* coordinate system; and take advantage of the formula depicted in equation (8). When $r^2 >> L^2 + R^2$, *i.e.*, point P is far away from the magnetic source, the field components can be simplified as equation (14):

$$\begin{cases} B_x = \dfrac{3\mu_0 P_m\sin\theta_0\cos\theta_0\cos\varphi_0}{4\pi r^3} \\ B_y = \dfrac{3\mu_0 P_m\sin\theta_0\cos\theta_0\sin\varphi_0}{4\pi r^3} \\ B_z = \dfrac{\mu_0 P_m}{4\pi r^3}(2 - 3\sin^2\theta_0) \end{cases}, \quad (14)$$

which is the same as the field of a dipole with magnetic moment P_m, located at position *O* and oriented along *Z*- axis. For example, at $r > 20L$, the error is within 5%.

III. Magnetically Tracking Method

Tracking of the marker is an inverse magnetic problem, in which the position and orientation of the marker are calculated based on the known distribution of the magnetic field. As shown in Fig. 2, the marker, which is modeled as a magnetic dipole, is located at an unknown position (x_0, y_0, z_0), with the unknown orientation angles (θ, φ); the ***N*** magnetic sensors, which are used to measure the magnetic field, are located at known position (x_i, y_i, z_i) (***i=1 to N***). The magnetic flux density around an arbitrary oriented dipole is expressed by equation (15):

$$\mathbf{B} = \frac{\mu_0}{4\pi}\left(-\frac{\mathbf{P_m}}{r^3} + \frac{3(\mathbf{P_m}\cdot\mathbf{r})\mathbf{r}}{r^5}\right), \quad (15)$$

where $\mathbf{P_m}$ is the magnetic moment vector of the dipole, and $\mathbf{r}$ is the spatial vector pointing from the dipole to the calculated point. As shown in Fig. 2, $\mathbf{P_m}$ can be written in the following form:

$$\mathbf{P_m} = p_m(\sin\theta\cos\varphi\mathbf{i} + \sin\theta\sin\varphi\mathbf{j} + \cos\theta\mathbf{k}), \quad (16)$$

in which p_m is the length of $\mathbf{P_m}$. And the spatial vector of the ***i*^th^** sensor is:

$$\mathbf{r}_i = (x_i - x_0)\mathbf{i} + (y_i - y_0)\mathbf{j} + (z_i - z_0)\mathbf{k} \quad (***i=1 to N***). \quad (17)$$

Substitute (16) and (17) into equation (15) and expand equation (15), we can express the three components of the magnetic field at the position of the ***i*th** sensor by equation (18):

$$B_{xi} = \frac{\mu_0 P_m}{4\pi r_i^5}\{M_x[2(x_i-x_0)^2-(y_i-y_0)^2-(z_i-z_0)^2]+ 3M_y(x_i-x_0)(y_i-y_0)+3M_z(x_i-x_0)(z_i-z_0)\}$$

$$B_{yi} = \frac{\mu_0 P_m}{4\pi r_i^5}\{M_y[2(y_i-y_0)^2-(x_i-x_0)^2-(z_i-z_0)^2]+ 3M_x(x_i-x_0)(y_i-y_0)+3M_z(y_i-y_0)(z_i-z_0)\} \quad , (18)$$

$$B_{zi} = \frac{\mu_0 P_m}{4\pi r_i^5}\{M_z[2(z_i-z_0)^2-(y_i-y_0)^2-(x_i-x_0)^2]+ 3M_x(x_i-x_0)(z_i-z_0)+3M_y(y_i-y_0)(z_i-z_0)\}$$

in which $r_i = |\mathbf{r_i}| = \sqrt{(x_i-x_0)^2+(y_i-y_0)^2+(z_i-z_0)^2}$, ***(i=1 to N)***

$M_x = \sin\theta\cos\varphi$, $M_y = \sin\theta\sin\varphi$, $M_z = \cos\theta$.

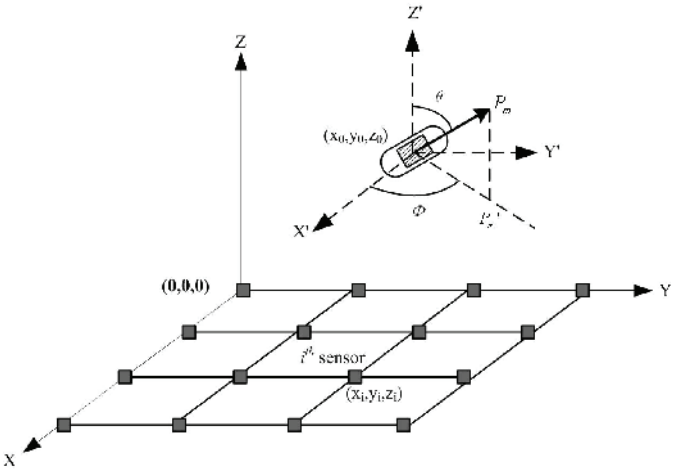

Fig.2 A magnet marker enclosed in the capsule, which is modeled as a dipole, moves in the coordinate of the sensor array.

The actual magnetic field components are measured by the sensors, which are noted as B_{mxi}, B_{myi}, and B_{mzi} (***i=1 to N***). The position and orientation of dipole can be obtained by minimizing the squared error between the values of calculation $B_{cal}^{(i)}$ and measurements $B_m^{(i)}$:

$$\min \sum_{i=1}^{N} (B_m^{(i)} - B_{cal}^{(i)})^2 \qquad (19)$$

The magnetic moment P_m can be pre-determined according to equation (1), so formula (19) consists of 5 unknown parameters $x_0, y_0, z_0, \theta, \varphi$. This problem can be solved by non-linear optimization algorithms, such as Powell's, downhill, DIRECT, multilevel coordinate search (MCS), and Levenberg-Marquardt (LM) algorithms. We find that LM algorithm is most suitable for our application [11] because of its high accuracy and non-sensitivity to the initial guess parameters.

IV. Experiments and Results

Based on the tracking method introduced in section III, we implement a real time localization system. As shown in the block diagram of Fig.3, the system consists of a sensor array, amplifiers (AD 623), a control circuit, a 16-channel USB based ADC (ZTIC-USB-7130, Beijing Zhongtai R&D limited), power supply and a computer (PII-233MHz). The pictures in Fig. 4 show a picture of the experimental setup. The sensors used in the system are Honeywell HMC1053 magneto-resistive sensors, each of which has three Wheatstone bridge elements to measure magnetic fields for both field strength and direction. The measurement range is ±6 Gauss with a resolution of 100μGauss. In addition to the bridge elements, this kind of sensors has two types of on-chip magnetically coupled straps: the offset strap, which allows for subtraction of an unwanted external magnetic field and nulling of the bridge offset voltage; and the set/reset strap, which is for incident field adjustment and magnetic domain alignment. The sensor array is composed of 16 3-axis magnetoresistive sensors, with an orthogonal distance of 75mm between every two adjacent ones. The coordinate system is the same as the one shown in Fig. 2.

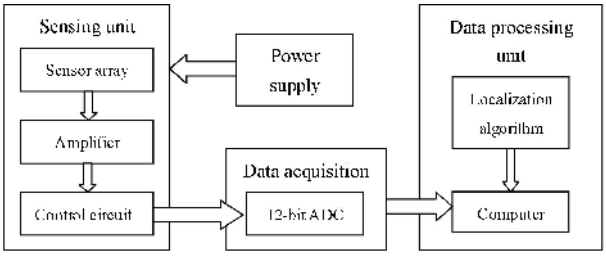

Fig. 3 Block diagram of experimental setup

The experiments were carried out in an ***unshielded*** room. The influence of the earth field is eliminated by using the offset strap. The magnetic marker used in this study was a Φ6×12mm cylindrical Nd-Fe-B permanent magnet. First, we fixed the magnet at a randomly selected position (-77.5mm, 49mm, 107.8mm) and orientation (0, 1, 0), and tested the localization accuracy with different number of sensors. As can be seen from Fig.5, when the measurement number is less than 8, the error is over 10mm, and the results are not satisfying. When the measurement number increases, the error decreases accordingly. After the measurement number reaches 15, the average error is stable at about 4mm and the average orientation error does not exceed 5%. Then we tested the 16-sensor system with different pre-determined orientations of the marker in a cuboid space (-120mm, -120mm to 120, 120mm with a height of 100mm above the sensor array). The average position error is 3.3mm (max 10mm), and average orientation error is about 3˚ (max 5.7˚).

As it's hard to measure the exact orientation of an arbitrary oriented magnet in a 3D space for comparison of the tracking results, we shaped the trajectory of the magnet by making it move in a plastic tube with a diameter of about 240mm, as shown in Fig. 6 (a1). The tube was placed above the sensor array with an average height of about 98mm. As can be seen from Fig. 6(a2), the tracking results exhibit the shape of the tube exactly. Then the magnet was placed 94mm above the sensor array and moved along straight lines. As shown in Fig. 6(b), the position results are satisfying within the sensor

area, while the error is getting larger beyond the area. It's obvious that the tracking lines outside the blue square are not as straight as those inside.

In this system, the tracking accuracy is improved by averaging the position and orientation of 100 samples. The execution time for a single point is 0.2-0.3s. When the moving speed of the magnetic marker is fast, the tracking results may become scattered points instead of continuous lines. For the capsule endoscope driven by natural peristalsis at a speed of 0.5mm/s, the response time of the system is short enough to make a real-time localization.

V. Conclusions

In this paper, a tracking method with 5 unknown parameters has been analyzed and implemented. The tracking system consists of a magnetic marker, 16 3-axis magnetoresistive sensors, data acquisition devices and a signal processing unit. The experiments were carried out in an unshielded environment. The results show that the system is robust and accurate when the magnet is moving within the range of the sensor array. Tracking with 16 sensors, the average position error is lower than 4mm, and the orientation error is within 5.7˚ when the marker is 100mm above the sensor array.

As the magnetic marker is very small, it can be enclosed into the capsule endoscope. The real-time system has great potential to be used for tracking the capsule during the procedure of capsule endoscopy.

References

[1] G. Iddan, G.Meron, A. Glukhovsky, and P. Swain, " Wireless capsule endoscopy", Nature, vol. 405, pp.717, 2000

[2] Doron Fischer, Reuven Schreiber, Daphna Levi, and Rami Eliakim, "Capsule endoscopy: the localization system", Gastrointestinal Endoscopy Clinics of North America, 14(2004), pp.25-31

[3] Eugene Paperno, Ichiro Sasada, and Eduard Leonovich, "A New Method for Magnetic Position and Orientation Tracking", IEEE Transactions on Magnetics, vol. 37, no. 4, pp.1938-1940, July 2001

[4] V. Schlageter, P.-A.Besse, R.S.Popovic, and P. Kucera, "Tracking system with five degrees of freedom using a 2D-array of hall sensors and a permanent magnet", sensors and actuators, A92, pp.37-42, 2001

[5] T. Nagaoka, A. Uchiyama, "Development of a small wireless position sensor for medical capsule devices", Proceedings of the 26th Annual International Conference of the IEEE EMBS, San Francisco, CA, USA, pp.2137-2140, September, 2004

[6] W. Weitschines, J. Wedemeyer, R. Stehr, and L. Trahms, "Magnetic marker as a noninvasive tool to monitor gastrointestinal transit", IEEE Transactions on Biomedical Engineering, vol. 41, no. 2, pp.192-195, February 1994

[7] N. Mani Prakash, Francis A. Spelman, "Localization of a magnetic marker for GI mobility studies: an in vitro feasibility study", Proceedings of 19th International Conference of IEEE/EMBS, pp.2394-2397, Chicago, USA, 1997

[8] Wilfried Andra, Henri Danan, Walter Kirmße, Hans-Helmar Kramer, Pieter Saupe, Rainer Schmieg and Matthias E Bellemann, "A novel method for real-time magnetic marker monitoring in the gastrointestinal tract", Phys. Med. Biol. 45, pp.3081–3093, 2000

[9] Yoshiaki Yamada, Noriaki Yoshida, Kazuhide Kobayashi, and Kiyotaka Yam, "An application of magnet and magnetic sensor: measurement system for tooth movement", IEEE Transactions on Biomedical Engineering, vol. 37, No. 10, pp.919-924, October 1990.

[10] S. Yabukami, H. Kanetaka, N. Tsuji, A. Itagaki, M. Yamaguchi, K. I. Arai, and H. Mitani, "A New Tracking System of Jaw Movement Using Two Magnets", IEEE Transactions on Magnetics, vol. 38, no. 5, pp.3315-3317, September, 2002

[11] Xiaona Wang, Max Q.-H. Meng, "Study of a position and orientation tracking method for wireless capsule endoscope", International Journal of Information Acquisition, vol.2, no.2, pp.113-121, 2005.

[12] Chao Hu, Max Q.-H. Meng, Mrinal Mandal, and Xiaona Wang, "3-axis magnetic sensor array system for tracking magnet's position and orientation", The 6th World Congress on Intelligent Control and Automation, accepted, Dalian, China, June 2006

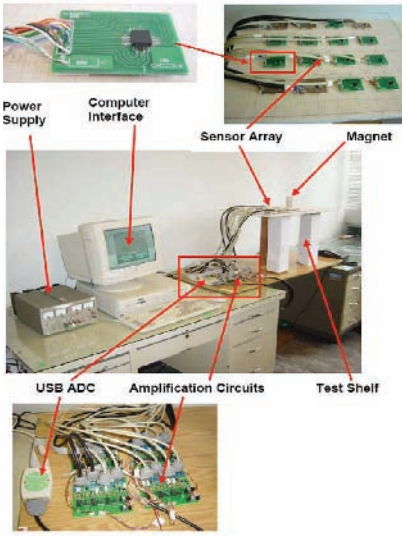

Fig. 4 Real-time localization system

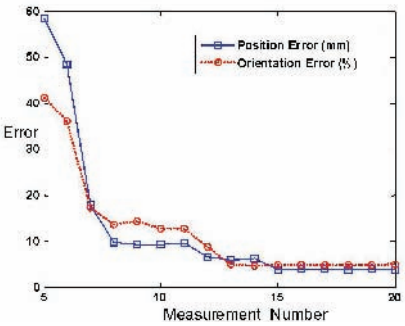

Fig. 5 Average position and orientation error vs. measurement number

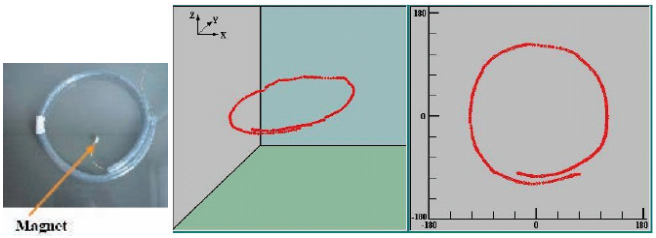

(a1) Picture of the plastic tube (a2) Tracking results of the tube

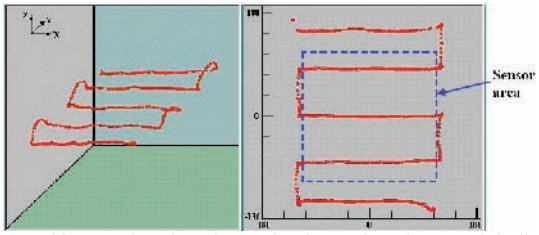

(b) Tracking results when the marker is moving along straight lines

Fig. 6 Real-time tracking results